scientific reports

Check for updates

OPEN

FGF6 inhibits oral squamous cell carcinoma progression by regulating PI3K/AKT and MAPK pathways

Xuan Zhang[1,2,6], Yingjiao Xu[2,3,6], Lijuan Shi[2,3], Xiao Chen[4,5], Miaoling Hu[2,3], Mengxue Zhang[2,3], Minhai Nie[2,3]✉ & Xuqian Liu[1,2]✉

To explore diagnostic and prognostic biomarkers in the progression of oral squamous cell carcinoma (OSCC) and to reveal their regulatory mechanisms in key pathways. A RayBiotech protein chip was used to screen differentially expressed serum proteins in OSCC, oral leukoplakia (OLK), and healthy participants. Gene Ontology (GO) and Kyoto Encyclopedia of Genes and Genomes (KEGG) enrichment analysis were used to determine the pathways enriched by characteristic differential proteins. Immunohistochemical analysis and western blotting were used to verify the expression of characteristic differential proteins and key regulatory factors in human tissues and in a nude mouse model. Fibroblast growth factor 6 (FGF6) was identified as a key differential protein and was weakly expressed in OSCC tissues. The mitogen-activated protein kinases (MAPK) and PI3K-AKT pathways were identified as key signaling pathways. The results showed that pERK, Cyclin D1, pAKT, and BCL2 were highly expressed in OSCC, Caspase9 was lowly expressed in OSCC. With an increase in FGF6 expression in nude mice, the expression of FGFR4, pERK, Cyclin D1, pAKT, BCL2, GPX4, and ACSL4 increased, and the expression of Caspase9 decreased. FGF6 may change the expression of apoptosis-related proteins and proliferation factors by binding to FGFR4 in the PI3K-AKT/MAPK pathway and may inhibit the ferroptosis of OSCC, thereby possibly participating in the process of inhibiting OSCC.

Keywords FGF6, OSCC, PI3K-AKT, MAPK, Ferroptosis

Oral squamous cell carcinoma (OSCC) is one of the most prevalent malignant tumors of the head and neck[1]. OSCC has received widespread attention due to its high prevalence, recurrence, mortality, and poor prognosis[2]. OSCC may develop from oral potentially malignant disorder (OPMD)[3]. OSCC is generally preceded by various OPMDs of which oral leukoplakia (OLK) is one of the most common OPMD[4]. Studies have shown that it can take years or longer to transition from OPMD to cancer[5]. Therefore, diagnosis and treatment of OPMD at this critical stage is an effective way to prevent and treat OSCC. Currently, the diagnosis of OSCC is primarily based on the pathological examination of living tissues. However, owing to its invasiveness, great postoperative impact, and heavy psychological burden on patients, the application of OSCC in disease screening and early diagnosis is limited[6,7]. Therefore, there is an urgent need for a minimally invasive method to diagnose OPMD. Liquid biopsy is used to sample body fluids, such as blood, urine, cerebrospinal fluid, or saliva[8,9], and to detect tumor biomarkers to obtain tumor-related information, which can be used for early diagnosis, efficacy evaluation, and follow-up of tumors[10,11]. It has the advantages of low sampling risk, low time consumption, convenient continuous sampling, and dynamic monitoring[12]. Among these, blood biopsies are the most widely studied[13].

Fibroblast growth factor (FGF) is a polypeptide family secreted by the pituitary gland and hypothalamus, and FGF6 is mainly expressed in skeletal muscle[14]. FGF6 is closely related to the development of tumor cells and plays an important role in their development and apoptosis of tumor cells[15,16]. Zhi et al. discovered that

[1]Department of Oral Basic Medicine, The Affiliated Stomatological Hospital of Southwest Medical University, Luzhou 646000, Sichuan, China. [2]Oral & Maxillofacial Reconstruction and Regeneration of Luzhou Key Laboratory, Southwest Medical University, Sichuan 646000, China. [3]Department of Periodontics & Oral Mucosal Diseases, The Affiliated Stomatological Hospital of Southwest Medical University, Luzhou 646000, Sichuan, China. [4]Department of Stomatology Technology, School of Medical Technology, Sichuan College of Traditional Medcine, Mianyang 621000, China. [5]Department of Orthodontics, Mianyang Stomatological Hospital, Mianyang 621000, China. [6]These authors contributed equally: Xuan Zhang and Yingjiao Xu. ✉email: nieminhaiwork@163.com; liuxuqianwork@163.com

overexpression of FGF6 reversed the inhibitory effect of LINC00265 knockdown on the malignant phenotype of bladder cancer cells[17]. Guo et al. further illuminated the role of FGF6 in modulating iron homeostasis, revealing its capacity to evoke transcriptional modulation of hepcidin[18]. Singhi et al. conducted targeted genome analysis of a large number of pancreatic ductal adenocarcinomas (PDAC) and found that FGF6 may be related to the pathogenesis of PDAC[19]. No study has shown that FGF6 can be used as a specific differential biomarker for all stages of OSCC.

The fibroblast growth factor receptor (FGFR) is a highly conserved and widely distributed transmembrane tyrosine kinase receptor, including FGFR1, FGFR2, FGFR3, and FGFR4 receptor subtypes[20]. Binding of FGF to FGFR causes intracellular phosphorylation of the receptor kinase domain and a cascade of intracellular signal transduction and gene transcription[21]. Dysregulation of FGFR signaling can lead to downstream activation of the mitogen-activated protein kinase (MAPK) and phosphoinositide-3-kinase (PI3K)/serine/threonine kinase (AKT) pathways[22]. The PI3K-AKT signaling pathway is closely related to the biological behavior of tumor cells and is an important anticancer therapeutic target[23]. It was confirmed that numerous oncogenes and growth factor receptors were shown to stimulate PI3K activity, and elevated PI3K signal was considered to be a hallmark of human cancer[24]. AKT, also known as protein kinase B, is an important effector of PI3K in the conduction of carcinogenic signals and participates in biological processes such as cell proliferation, apoptosis, and protein synthesis[25]. The PI3K-AKT signaling pathway has been established as a pivotal player in OSCC, with its downstream regulatory factors BCL2 and Caspase9 likewise implicated in tumor progression[26–28]. MAPK-ERK pathway has been proved to be an important signaling pathway involved in cancer cell proliferation[29]. MAPK interact with ERK, transduce extracellular signals, regulate the cell cycle, transmit cell proliferation signals, stimulate the expression of cell cycle-related proteins (Cyclin D1), and lead to cell proliferation cycle disorders[30]. Su et al. found that vitamin C can lead to BRAF mutations and resist thyroid cancer by inhibiting the transmission of MAPK-ERK and PI3K-AKT signals[31]. Ferroptosis is also closely related to the occurrence and development of malignant tumors such as breast cancer, gastric cancer, and OSCC[32–34].

In this study, a model of OSCC was established. The differentially expressed proteins and their possible signaling pathways were screened using RayBiotech protein chip technology and bioinformatics technology, and verified in human serum and tissue samples and animal models. It also focused on the key proteins in the ferroptosis pathway, aiming to explore the effect of FGF6 on differential proteins in the process of OSCC and provide new ideas for effectively delaying the process of OSCC.

Materials and methods

Collection of serum samples and experimental animals

Fresh serum and tissue samples of patients with OSCC, OLK, and normal serum and tissues were obtained from the Affiliated Stomatological Hospital of Southwest Medical University. Serum was collected from 33 OSCC patients, 10 with OLK patients and 16 healthy participants (Supplementary Table 1). Tissues were collected from 46 OSCC patients, 10 with OLK patients and 15 healthy participants (Supplementary Table 2). Inclusion criteria: None of the patients with OSCC or OLK received preoperative chemoradiation and chemotherapy and did not receive clinical intervention such as drugs within six months. Patients with other malignant tumors, oral mucosal diseases, or serious systemic diseases were excluded. Each patient was informed of the behavior and provided written informed consent. This study was approved by the Medical Ethics Committee of the Affiliated Stomatological Hospital of Southwest Medical University (approval number 20180510001). All experiments were performed in accordance with relevant named guidelines and regulations.

Male nude mice (3 to 4 weeks of age, weight about 12 g) were purchased from Beijing Huafukang Experimental Animal Co., Ltd. (Certificate No.: SCXK (Beijing) 2019-0008) and raised in SPF environment of the Experimental Animal Center of Southwest Medical University. The feed, bedding material, squirrel cage, kettle and drinking water of nude mice were all sterilized by high temperature and high pressure. The study is reported in accordance with ARRIVE guidelines. All animals were anesthetized and sedated with sodium pentobarbital (0.5% sodium solution of pentobarbital was intraperitoneally injected with 0.5mL/100 g). Research investigators choose to euthanize mice by cervical dislocation. This animal study was approved by the Southwest Medical University Animal Ethics Committee (ethical number 2020435). All experiments were performed in accordance with relevant named guidelines and regulations. The study is reported in accordance with ARRIVE guidelines.

Cell lines and culture

The human OSCC line (HSC-4) was purchased from Shenzhen Haodi Huatuo Biotechnology Co., LTD. The human immortalized keratinocyte cell line (HaCaT) was purchased from Wuhan Punosai Life Technology Co., Ltd. Cells were cultured in DMEM (Procell, China) with 15% (bove serum albumin BSA (Thermo Fisher Scientific, USA) and 1% penicillin-streptomycin solution (Beyotime, China) at 37 °C and 5% CO_2.

Cell transfection and animal model construction

The lentiviral vector for FGF6 overexpression was constructed by OBiO Technology Corp., Ltd. (Shanghai, China). The lentivirus was transfected into 96-well plates containing polybrene. The appropriate multiplicity of infection (MOI) and puromycin concentration were selected according to the cell growth state (HSC-4 cells: MOI = 60, puromycin concentration = 2 μg/mL; HaCaT cells: MOI = 40; puromycin concentration = 1 μg/mL). HSC-4 cells with good growth status and 80% cell density were inoculated in 6-well plates and cultured in a 5% CO_2 incubator at 37 °C for 24 h. FGF6 overexpression lentivirus and empty vector lentivirus were added to 6-well plates for cell transfection, and the blank group was set up. RT-qPCR was performed to verify the effect of lentivirus overexpression. Primer sequences are shown in Supplementary Table 3.

The experiment was simulated in three stages (Supplementary Fig. 1), each of which included FGF6 lentivirus transfection group and control group, respectively, with 6 nude mice in each group, a total of 36 mice.

At the normal stage, the HaCaT cell suspension (2×10^6 counts) transfected with FGF6 lentivirus was injected subcutaneously into the right back of nude mice as the FGF6 lentivirus transfection group, and the HaCaT cell suspension transfected with empty vector lentivirus was injected into the control group. In OLK stage, HaCaT cell suspension was injected subcutaneously into the right back of nude mice. After the formation of a stable epithelial-like structure, the FGF6 lentivirus transfection group was injected with HSC-4 cell suspension (2×10^6 counts) transfected with FGF6 lentivirus in the basement membrane area of the epithelial-like layer, and the control group was injected with HSC-4 cell suspension transfected with empty vector lentivirus. In OSCC stage, the HSC-4 cell suspension transfected with FGF6 lentivirus was injected subcutaneously into the right back of nude mice in the FGF6 lentivirus transfection group, and the HSC-4 cell suspension transfected with empty vector lentivirus was injected into the control group.

RayBiotech protein chip technology, bioinformatics analysis

The serum samples of OSCC, OLK, and normal tissues were analyzed using a protein chip to screen for differential proteins. Hierarchical clustering, Gene Ontology (GO), and Kyoto Encyclopedia of Genes and Genomes (KEGG) enrichment analyses were performed on the screened differential proteins using R Programming Language[35–37].

Real time quantitative PCR analysis

Total RNA was extracted using TRIzol reagent, and the concentration was determined using enzyme calibration (BioTek, Synergy HTX, USA). Total RNA was reverse-transcribed to cDNA using the All-in-One First-Strand Synthesis MasterMix kit (Sheng share, China). Real-time PCR was performed with SYBR Green PCR Master Mix on a Veriti 96 well PCR amplifier (Thermo Fisher Scientific, USA). The relative mRNA expression was calculated using the $2^{-\Delta\Delta Ct}$ method.

Histomorphological observation and HE staining

Fresh tissue samples were fixed in 10% formalin for 24 h and dehydrated with absolute ethanol. Five μm thick) were obtained from tissues included in paraffin blocks. The sections were stained in hematoxylin solution (BASO, China) for 5 min, differentiated in 1% acid alcohol for 1 s, treated with 1% ammonia for 1 min, counterstained with eosin solution (BASO, China) for 1 min, dehydrated in 70% alcohol, 80% alcohol, 95% alcohol, and mounted with neutral balsam (Solarbio, China). Multiple images of the sections were obtained using a orthostatic microscope (BX43, OLYMPUS, Japan).

Immunohistochemical (IHC) staining

Paraffin Sect. (5 μm) were deparaffinized and treated with alcohol. Sections were incubated overnight with primary antibodies at 4 °C. The sections were then washed three times with PBS. The sections were then incubated with the secondary antibody at room temperature for 15 min. The color was revealed by DAB and all sections were examined and photographed under a microscope (BX43, OLYMPUS, Japan).

Western blot assay

Proteins in the serum and tissue samples were extracted, and their concentrations were determined using a BCA kit (Solarbio, China). The total protein was separated and transferred to a PVDF membrane. The membrane was incubated with the primary antibody overnight at 4 °C: AKT1/2/3 (Abways, Beijing, 1:2000); BCL2 (Abways, Beijing, 1:1000); Phospho-AKT (Thr308) (Zenbio, Chengdu, 1:1000); Cyclin D1 (Zenbio, Chengdu, 1:1000); ERK1 + ERK2 (Bioss, Beijing, 1:2000); Capase 9 (Abways, Beijing, 1:2000); FGF6 (Bioss, Beijing, 1:1000); FGFR4 (Bioss, Beijing, 1:2000); FGFR1 (Bioss, Beijing, 1:1500); PI3K (Bioss, Beijing, 1:1000); ACSL4 (Abways, Beijing, 1:2000); GPX4 (Abways, Beijing, 1:2000); GAPDH (Affinity, Shanghai, 1:50000); Phospho-ERK1/2 (Bioss, Beijing, 1:2000). And then incubated with the Goat Anti-Rabbit IgG H&L antibody (Bioss, China, 1:50000) at room temperature for 1 h. The membrane was washed three times with TBST and then incubated with ECL solution (Sheng share, China) for 2 min in the dark and photographed using a microscopic imaging system (Invitrogen, iBright CL 1000, USA).

Determination of malondialdehyde (MDA) and Fe^{2+} content

The MDA content was detected using an MDA detection kit (Solarbio, China) according to the manufacturer's instructions. Fe^{2+} levels were measured using a Ferrous Iron Colorimetric Assay Kit (Elabscience, China) according to the manufacturer's instructions.

Statistical analysis

SPSS20.0 was used for statistical analysis, one-way analysis of variance (One-Way ANOVA), t-test, and Kruskal-Wallis H Test were used to analyze the data. GraphPad Prism9 was used to create the diagram. In the graphs, ns indicates $P > 0.05$, $P < 0.05$ was as statistically significant. ($^*P < 0.05$, $^{**}P < 0.01$, $^{***}P < 0.001$, $^{****}P < 0.0001$, Values are presented as means ± standard error).

Results

Analysis of differential proteins expression

Three serum samples were randomly selected from the OSCC, OLK, and normal groups for the RayBiotech protein chip detection. The results showed differentially expressed proteins among the three groups (Fold Change > 2, $P < 0.05$). The expression of FGF6 is significant different between the OSCC and normal groups and between the OSCC and OLK groups (Fig. 1A). Therefore, FGF6 is considered the main target of research to verify its role in OSCC. A heat map of the differentially expressed proteins is shown in Fig. 1B–D.

A

	Protein	Fold Change	Regulation
OSCC *vs* OLK group	NT4	6.19	up
	FGF6	63.308	up
	BAFF	55.24	up
	Pepsinogen	1.84	up
	Decorin	1.65	up
OSCC *vs* normal group	MMP3	11.62	up
	FGF6	307.79	up
	Angiostatin	2.27	up
	I309	69.57	up
	AgRp	2.55	up
	Mer	346.99	up
OLK *vs* normal group	MMP3	6.153	up
	CTACK	6.04	up
	GDF15	8.67	up

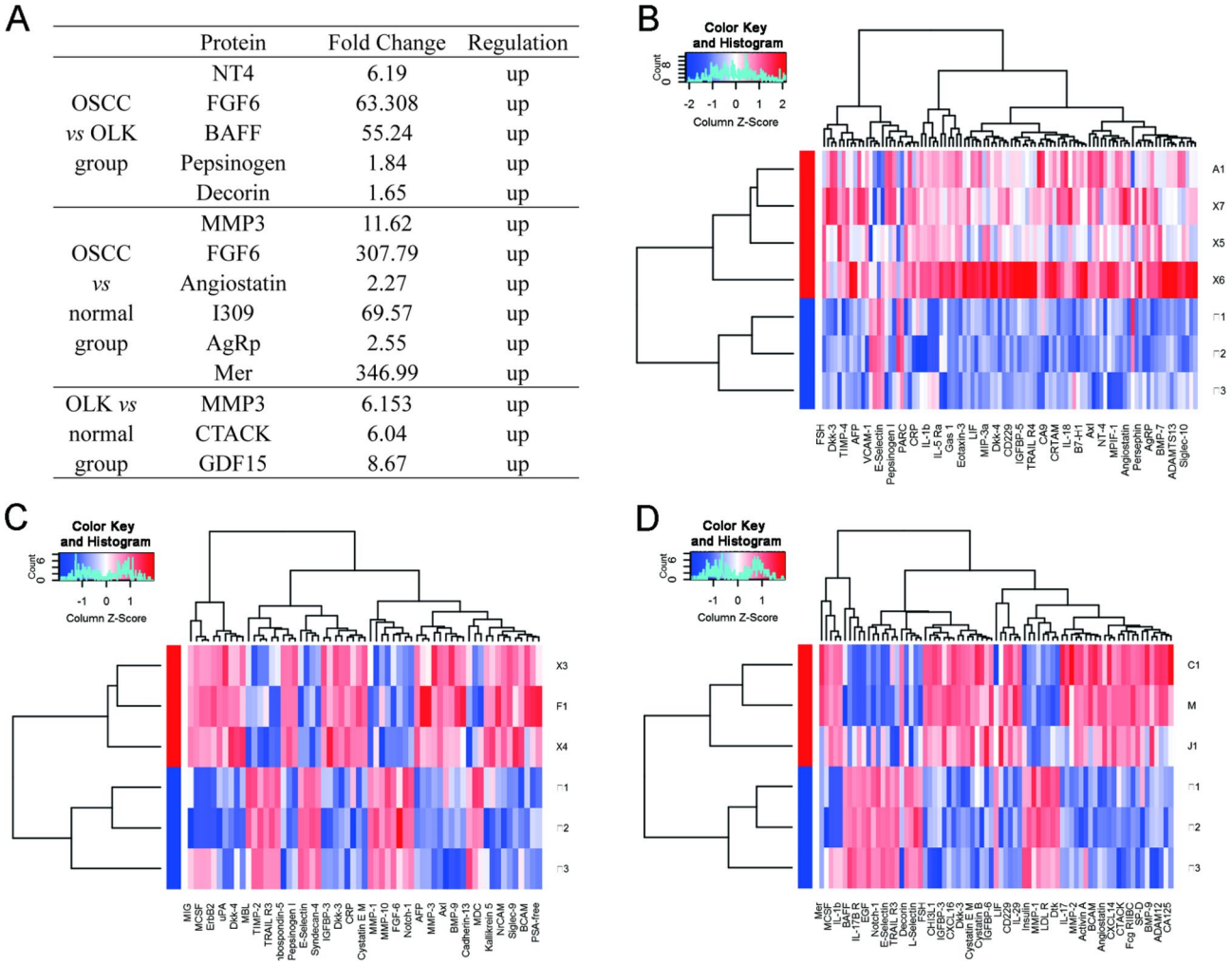

Fig. 1. Analysis of differential proteins expression and heat map of differentially expressed proteins. (**A**) Differentially expressed proteins between OSCC and OLK group, between OSCC and normal group and between OLK group and normal group. (**B**) Differentially expressed proteins between OSCC and normal group in heat map. (**C**) Differentially expressed proteins between OSCC and OLK group in heat map. (**D**) Differentially expressed proteins between OLK and normal group in heat map.

Functional enrichment analyses of the differential proteins

GO and KEGG enrichment analysis were used to screen the functional characteristics of differential proteins and their involved signaling pathways. The differential proteins in the OSCC group compared with the normal group were mainly involved in biological processes, such as lymphocyte chemotaxis, mononuclear cell migration, and monocyte chemotaxis, and were mainly enriched in viral protein interactions with cytokines and cytokine receptors, cytokine-cytokine receptor interactions, and other pathways (Fig. 2). The differentially expressed proteins in the OSCC group compared with the OLK group were mainly involved in biological processes, such as response to interleukin-17, interleukin-17-mediated signaling pathway, and cellular response to interleukin-17, and were mainly enriched in the renin-angiotensin system, interleukin-17 signaling pathway, and other pathways (Fig. 3). The differentially expressed proteins in the OLK group compared with the normal group were mainly involved in biological processes, such as lymphocyte chemotaxis, mononuclear cell migration, and extracellular matrix disassembly, and were mainly enriched in viral protein interactions with cytokines and cytokine receptors, rheumatoid arthritis, and other pathways (Fig. 4). According to the classical signaling pathways of cell proliferation and apoptosis and combined with KEGG enrichment analysis, we selected the signaling pathways involved in FGF6, including the MAPK and PI3K-AKT pathways.

Different expression of key regulatory factors in serum of OSCC group, OLK group and normal group

We investigated the differences in the expression of key regulatory factors in the above pathways in the serum of OSCC, OLK, and normal groups using western blotting. As shown in Fig. 5A, B shown, the expression of FGF6 in the serum of the OSCC group was significantly higher than that in the OLK and normal groups. The expression of FGFR4 and FGFR1 in the serum of the OSCC group was significantly higher than that of the

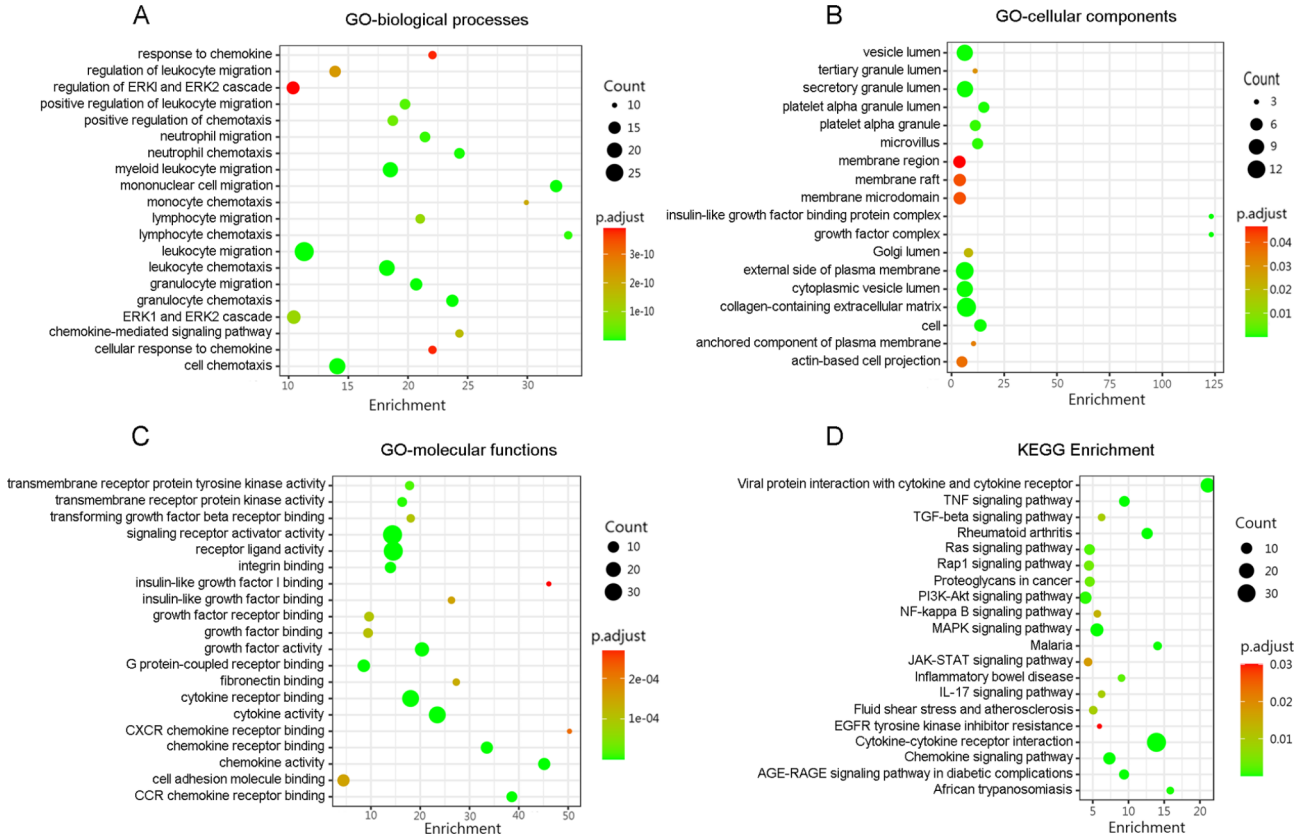

Fig. 2. The main biological processes, cellular components, molecular functions and signaling pathways involved in differential proteins in OSCC and normal group were analyzed.

normal group. In the MAPK pathway, there was no significant difference in the expression of ERK in the three serum groups. The expression of pERK in the OSCC group was significantly higher than that in the OLK and control groups. The expression of BRAF and cyclin D1 was significantly higher in the OSCC group than in the normal group. In the PI3K-AKT pathway, the expression of PI3K, pAKT, Caspase9, and BCL2 was significantly higher in the OSCC group than in the normal group. There was no significant difference in the expression of AKT between the three serum groups. There was no significant difference in the expression of the ferroptosis-related genes GPX4 and ACSL4 in the serum of the OSCC, OLK, and normal groups.

Different expression of key regulatory factors in tissues of OSCC group, OLK group and normal group

IHC results showed that the expression of FGF6 in tissues of the OSCC group was significantly lower and that of FGFR4 in tissues of the OSCC group was significantly higher than that in the OLK and normal groups (Fig. 6A, B). There was no significant difference in the expression FGFR1 among the three groups of tissues. In the MAPK pathway, there was no significant difference in the expression of BRAF and ERK among the three groups of tissues. The expression levels of pERK and Cyclin D1 in OSCC group were significantly higher than those in the OLK and normal groups. In the PI3K-AKT pathway, there was no significant difference in the expression of AKT and PI3K among the three groups of tissues. The expression levels of pAKT and BCL2 in the OSCC group were significantly higher than those in the OLK and normal groups. The expression of Caspase9 in the OSCC group was significantly lower than that in the normal group. The expression of the ferroptosis-related genes GPX4 and ACSL4 was significantly higher in the OSCC group than in the normal group.

Western blotting results showed that the expression of FGF6 in tissues of the OSCC group was significantly lower than that in the OLK and normal groups. There was no significant difference in the expression of FGFR1 between the three groups of tissues. The expression of FGFR4 in OSCC group was significantly higher than that in normal group. The expression of regulatory factors in MAPK and PI3K-AKT signaling pathways and ferroptosis-related genes GPX4 and ACSL4 was consistent with the IHC results (Fig. 7A, B).

Effect of overexpression of FGF6 on OSCC xenografts

We verified the effect of FGF6 overexpression by RT-qPCR (Fig. 8A). Compared with the blank group, the relative expression of FGF6 in HSC-4 cells was significantly higher in the FGF6 lentivirus transfection group (OE group). There was no significant difference in the expression of FGF6 between the blank and control groups.

Lentivirus interferes with the process of OSCC disease model as shown in Fig. 8B, C, the FGF-6-overexpression precancerous lesion tissue group showed a tumorigenic trend and tended to be histopathologically characterized

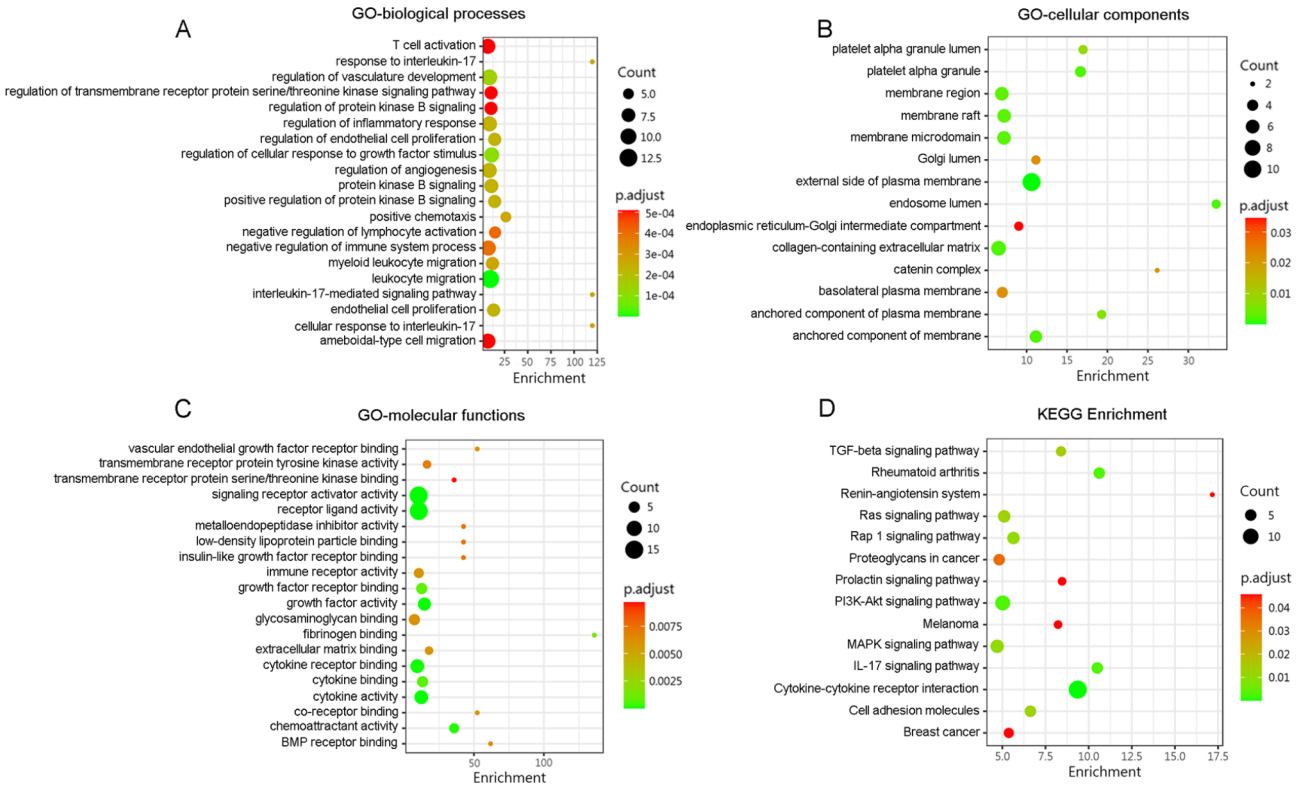

Fig. 3. The main biological processes, cellular components, molecular functions and signaling pathways involved in differential proteins in OSCC and OLK group were analyzed.

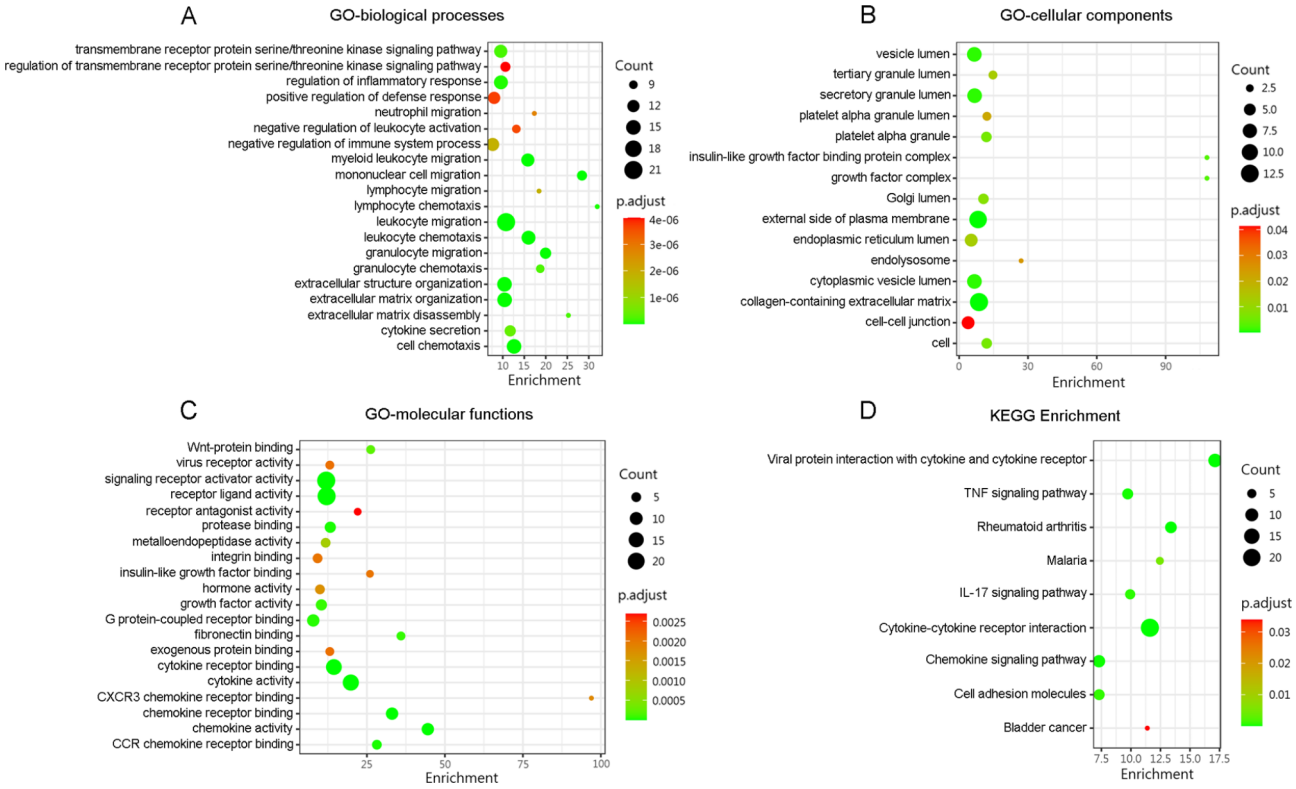

Fig. 4. The main biological processes, cellular components, molecular functions and signaling pathways involved in differential proteins in OLK and normal group were analyzed.

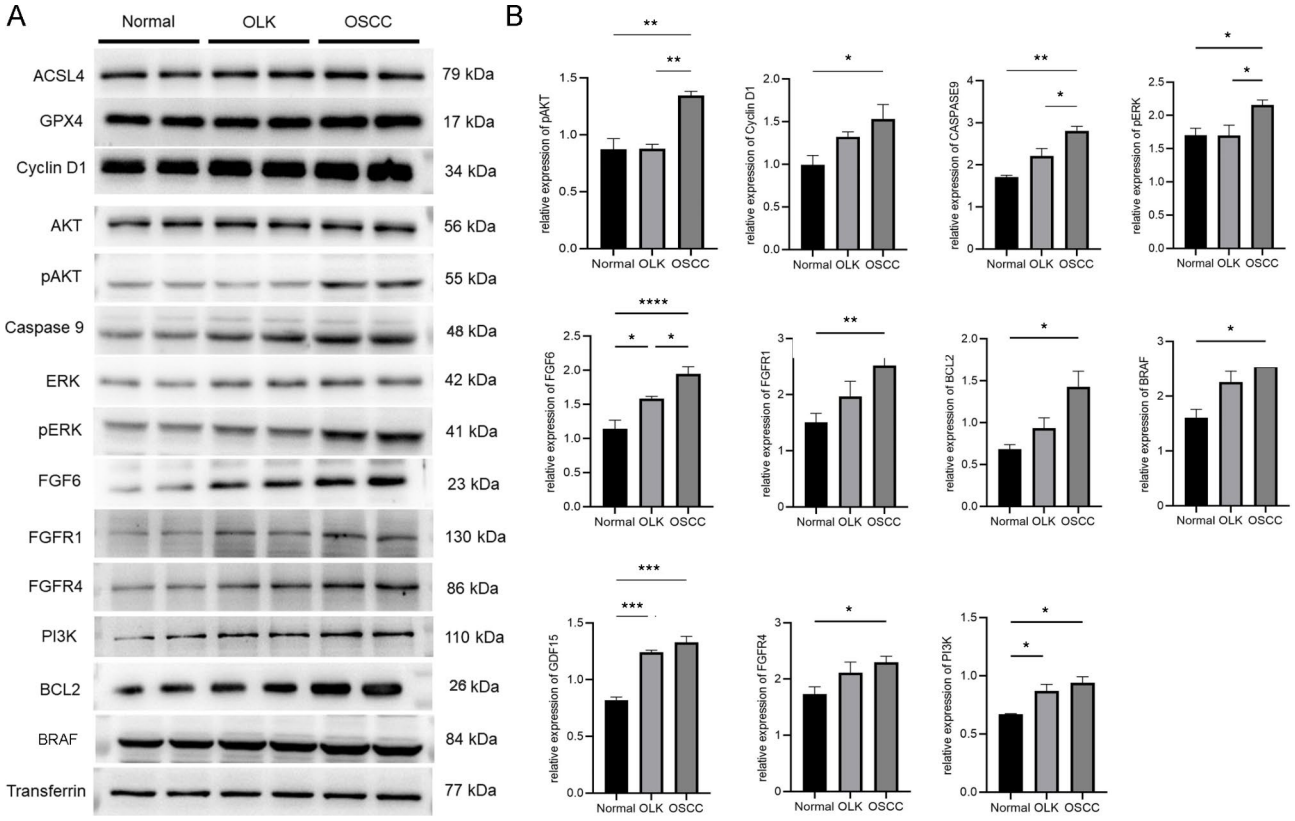

Fig. 5. Different expression of key regulatory factors in serum of OSCC group, OLK group and normal group. (**A**) Results of serum Western Blot (Original blots/gels are presented in Supplementary information). (**B**) Gray value statistics. Statistical analysis was performed using the independent sample t-test. $^{*}P < 0.05$ $^{**}P < 0.01$ $^{***}P < 0.001$.

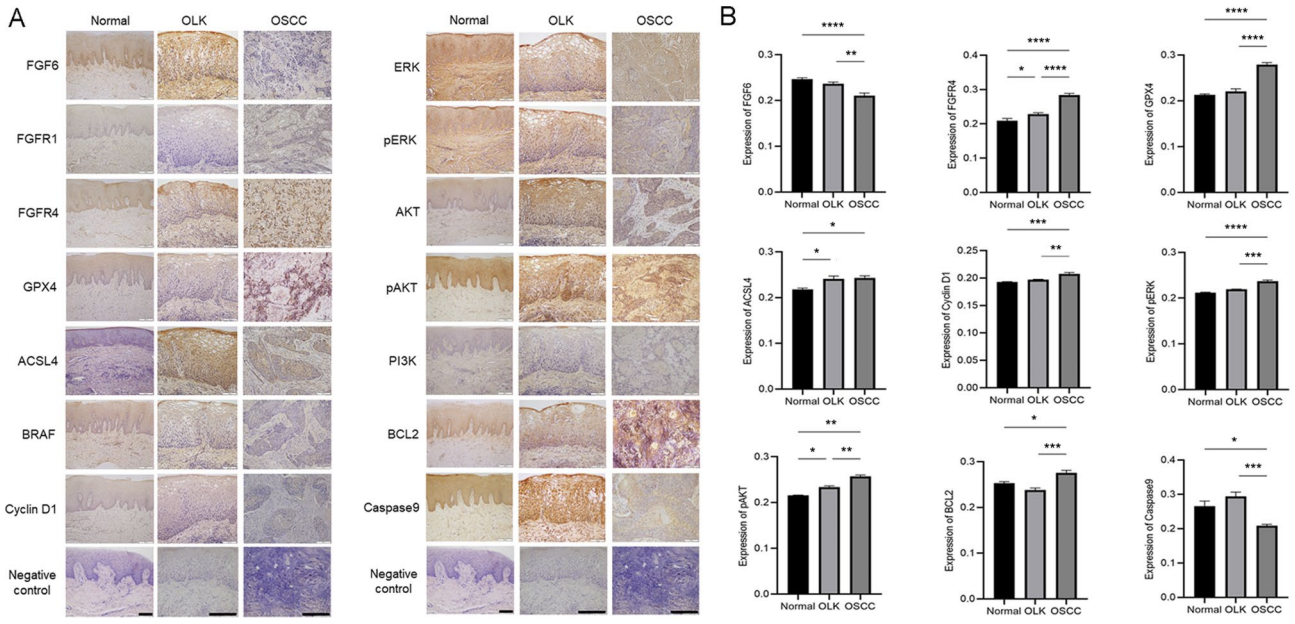

Fig. 6. Different expression of key regulatory factors in tissues of OSCC group, OLK group and normal group. (**A**, **B**) IHC results. bar = 200 μm OSCC and OLK group (×200) normal group (×100) $n \geq 3$ Statistical analysis was performed using the independent sample t-test. $^{*}P < 0.05$ $^{**}P < 0.01$ $^{***}<0.001$ $^{****}P < 0.0001$.

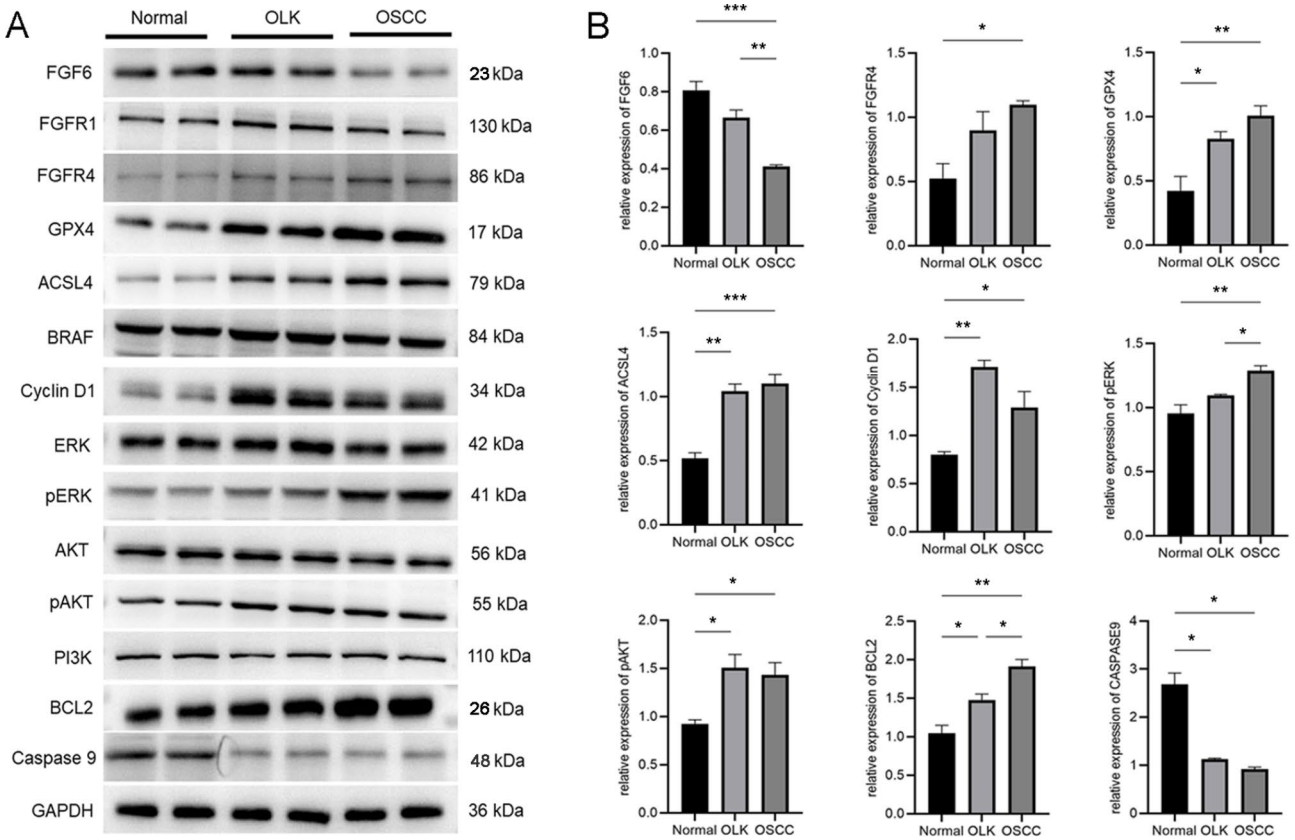

Fig. 7. Different expression of key regulatory factors in tissues of OSCC group, OLK group and normal group. (**A**, **B**) Western blot results (Original blots/gels are presented in Supplementary information). Statistical analysis was performed using the independent sample t-test. $^{*}P<0.05$ $^{**}P<0.01$ $^{***}P<0.001$.

by OSCC. In the mucosal carcinogenesis stage, the tumor in the FGF-6-overexpression group was higher than that in the control group (Fig. 8B, C). The degree of differentiation of tumor-bearing OSCC tissue in nude mice of the FGF-6-overexpression group was lower than that in the control group, and there was a large area of necrotic tissue (Fig. 8D).

Exploring the different expression of key regulatory factors in vivo

We explored the effects of FGF6 overexpression on key regulatory factors in normal, precancerous, and cancer tissues. IHC results showed that the expression of FGF6 was significantly higher in the OE group than in normal, precancerous, or cancer tissues (Fig. 9and Supplementary Fig. 2). The expression of FGF6 was significantly lower in cancer tissues in both control and OE groups. The expression of FGFR4 was significantly higher in cancer tissues in both control and OE groups. There was no significant difference in the expression FGFR1 between the groups. In the PI3K-AKT pathway, the expression of BCL2 was significantly higher and of Caspase9 was significantly lower in the OE group than in normal, precancerous, or cancer tissues. There were no significant differences in the expression levels of PI3K and AKT between the groups. In the MAPK pathway, the expression of pERK and Cyclin D1 was significantly higher in the OE group than in the precancerous or cancer tissues. There were no significant differences in ERK expression between the groups. The expression of ferroptosis-related genes GPX4 and ACSL4 was significantly higher in the OE group than in the normal, precancerous, or cancer tissues.

Western blotting results showed that the expression of FGF6 was significantly higher in the OE group than in normal tissues, precancerous tissues, or cancer tissues (Fig. 10and Supplementary Fig. 3). The expression of FGFR4 was significantly higher in cancer tissues than in the control group. There was no significant difference in the expression FGFR1 between the groups.

In the PI3K-AKT and MAPK pathway, the expression of key regulatory factors was consistent with IHC results. The expression of the ferroptosis-related genes GPX4 and ACSL4 was also consistent with the IHC results.

Content of MDA and Fe^{2+} in vitro and in vivo

The MDA and Fe^{2+} contents in the OSCC group were significantly lower than those in the OLK and normal groups in vitro (Fig. 11A, B). The contents of MDA and Fe^{2+} in cancer tissues were significantly lower than those in normal and precancerous tissues in vivo. The levels of MDA and Fe^{2+} in the OE group were significantly lower than those in the control group (Fig. 11C–L).

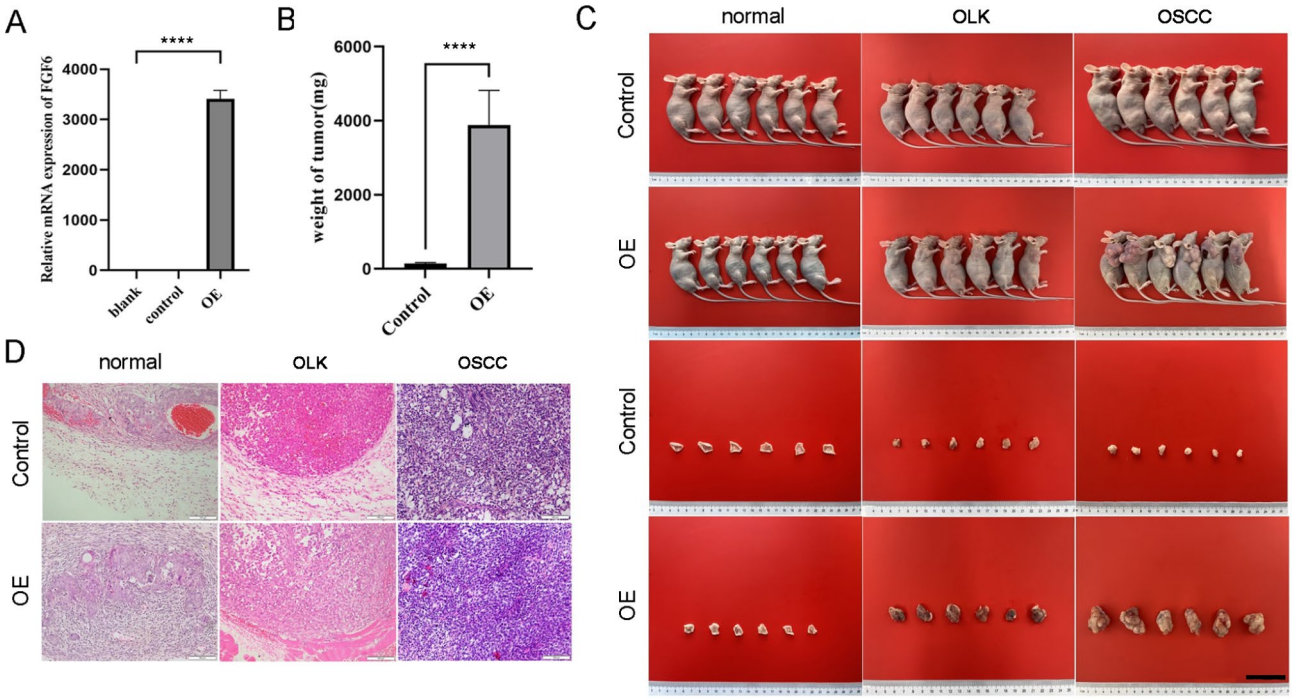

Fig. 8. Nude mouse model construction results (**A**) The relative expression of FGF6 in HSC-4 after transfection with lentivirus. Statistical analysis was performed using the independent sample t-test. $^{****}P < 0.0001$ (**B**) Weight difference of subcutaneous tumor in the mucosal carcinogenesis stage. Statistical analysis was performed using the independent sample t-test. $^{****}P < 0.0001$ (**C**) The animal modeling in general. bar = 5 cm (**D**) HE staining results. (×200) bar = 100 μm.

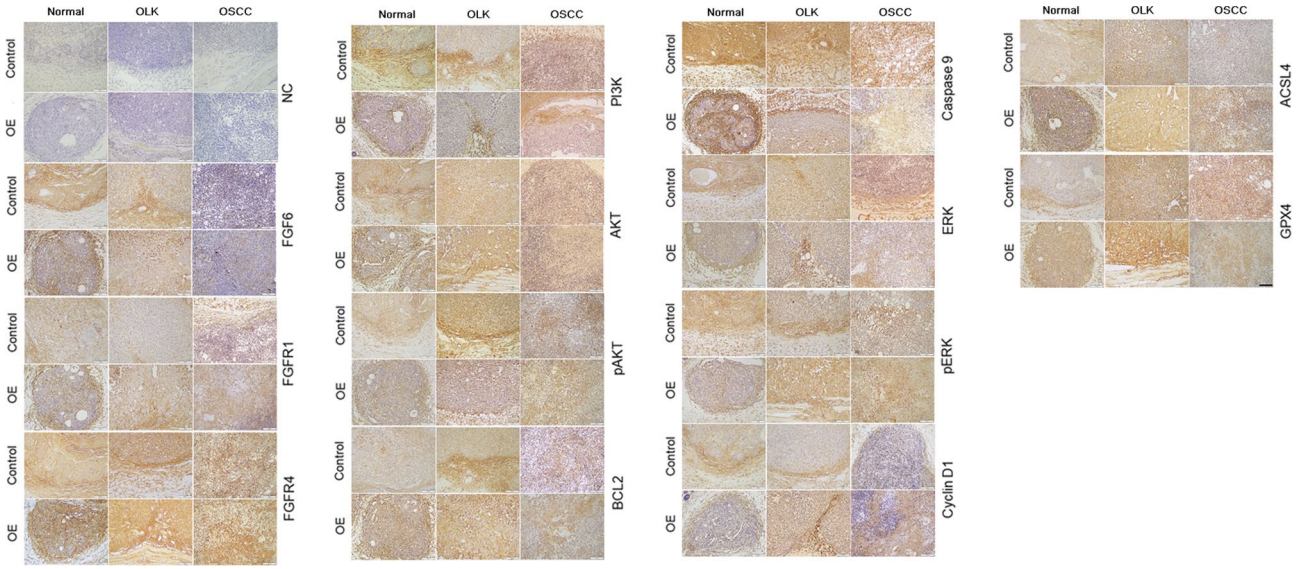

Fig. 9. Different expression of key regulatory factors in vivo. IHC results. (×200) bar = 100 μm $n \geq 3$.

Discussion

FGF6 is a secreted protein, the human FGF6 gene is located on chromosome 12p13. Its cleavable N-terminal signal peptide functions as an extracellular medium, facilitating the binding and activation of FGFR. Penault-Llorca et al. detected the expression of FGF6 in 15% of breast cancer cases[38]. In the research of Kwabi-Addo et al., neither normal prostate nor breast tissues showed any signs of FGF6 expression[39]. The above studies have shown that FGF6 is highly expressed in other squamous cell carcinomas and adenocarcinoma tissues. This result is inconsistent with our verification results of FGF6 in proteomics and tissue sample expression

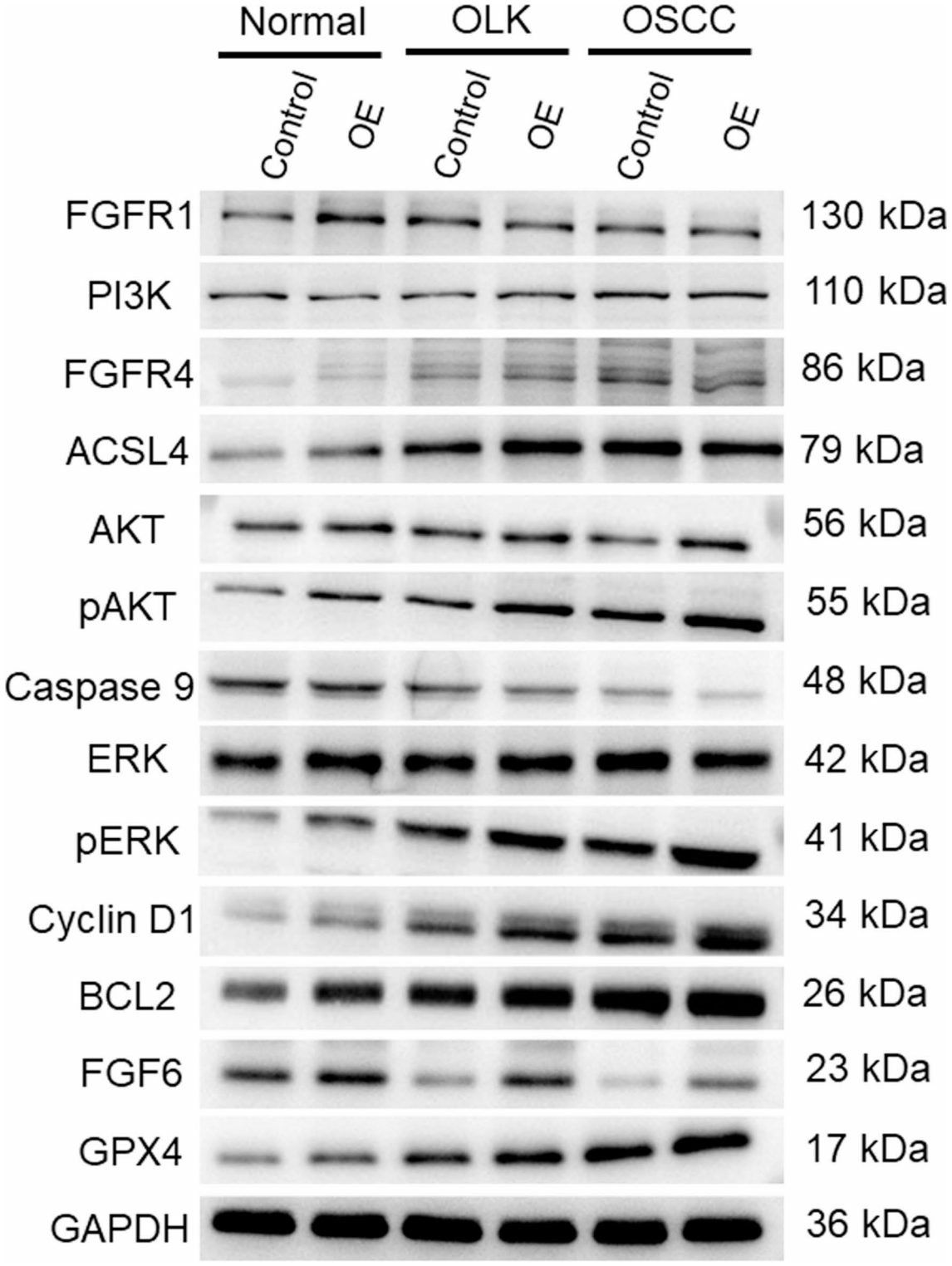

Fig. 10. Different expression of key regulatory factors in vivo. Western blot results (Original blots/gels are presented in Supplementary information).

in OSCC, suggesting that FGF6 may not have been recognized in previous studies as a specific biomarker for different stages of OSCC. Our results showed that the expression of FGF6 in the serum of the OSCC group was higher than that in the OLK and normal groups. However, tissue samples showed that FGF6 was highly expressed in the normal group. The reason might be that FGF6 stimulates the growth of vascular endothelial cells by promoting angiogenesis, thereby releasing growth factors and causing changes in vascular endothelial cell permeability[40]. Besides, the neovascularization can promote the proliferation and differentiation of tumor

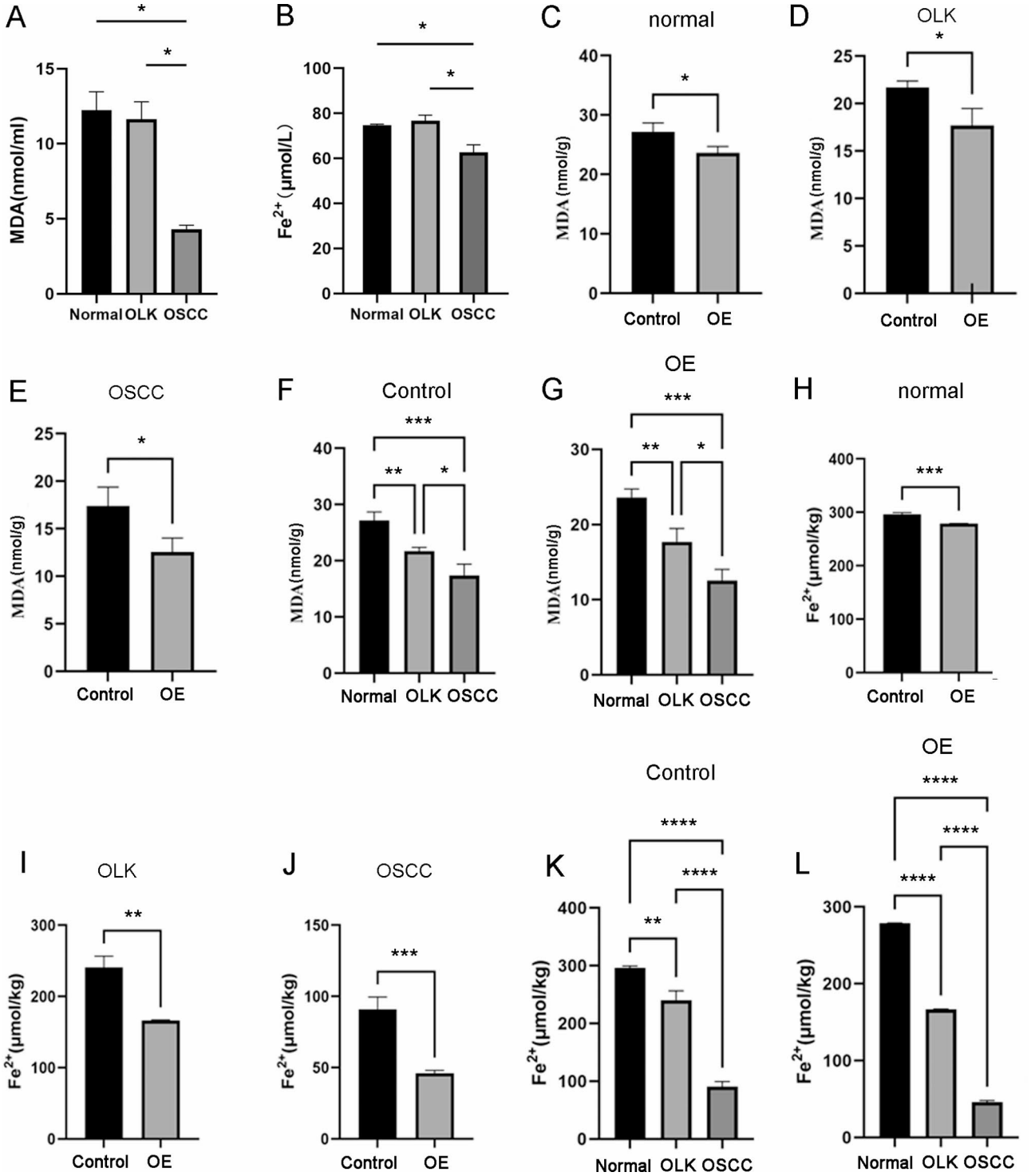

Fig. 11. Content of MDA and Fe^{2+}in vitro an in vivo (**A**) The content of MDA in vitro. (**B**) The content of Fe^{2+} in vitro. (**C**–**G**) The content of MDA in vivo. (**H**–**L**) The content of Fe^{2+} in vivo. Statistical analysis was performed using the independent sample t-test. $^{*}P<0.05$ $^{**}P<0.01$ $^{***}P<0.001$ $^{****}P<0.0001$.

cells[41]. The proliferation of new blood vessels in tumors may lead to vascular leakage, that is, tumor cells may invade new microvessels through the permeability change of vascular endothelial cells in the late stage of cancer, and continue to grow until they reach a new site[42]. This results in increased expression of FGF6 in serum due to changes in vascular endothelial cell permeability.

We found that FGFR4 and FGFR1, receptors that bind to FGF6 in the enrichment pathway, were highly expressed in the serum of the OSCC group. FGFR4 was highly expressed in OSCC tissues. There was no significant difference in the expression of FGFR1 in the normal, OLK, and OSCC groups, indicating that FGFR4

may be involved in downstream proteins of the regulatory pathway as a key receptor binding to FGF6 in the regulation of OSCC.

The phosphorylation level of AKT was upregulated in the control normal tissues, control precancerous tissues, and control cancer tissues, while the expression levels of PI3K and AKT were not statistically significant among the three groups, indicating that FGF6 may accelerate the carcinogenesis of OPMD by promoting AKT phosphorylation. The upregulation of BCL2 expression was observed consistently across the control normal tissues, precancerous tissues, and cancer tissues, concomitantly with an increase in Caspase9 protein levels. This indicates that FGF6 exerts its influence by potentially binding to either FGFR4 or FGFR1, engaging in the PI3K-AKT signaling cascade. This interaction triggers AKT phosphorylation, leading to an upregulation of BCL2 and a corresponding downregulation of Caspase9, thereby implicating FGF6 in the inhibition of cancer cell apoptosis. As previously reported, decreased BCL2 expression is associated with good cell differentiation and prognosis in OSCC[43,44]. Knockdown of chloride intracellular channel 1 can downregulate the expression of pERK and upregulate the expression of Caspase9, which can inhibit the proliferation, migration, and invasion of OSCC cells, thus promoting tumor cell apoptosis[28]. Our results showed that pERK expression was upregulated with the upregulation of FGF6 protein expression, whereas ERK expression remained unchanged. This suggested that FGF6 may stimulate the MAPK pathway and promote ERK phosphorylation by binding to FGFR4. The upregulation of Cyclin D1 expression concurred with FGF6 protein expression, suggesting a mechanistic link wherein FGF6 triggers ERK phosphorylation through the MAPK signaling cascade. This orchestrated event ultimately enhances the expression of Cyclin D1, thereby fostering the proliferation of cancer cells. The discrepancy between the mRNA expression levels of FGFR4, FGF6 and Caspase9, and their respective protein expression levels, can be attributed to the inherent instability of the transcriptome, resulting in the potential loss of certain information. This showed that their expression at the protein level is inconsistent with the expression at the transcriptional level.

Sun et al. found that overexpression of miR-34c-3p in SCC-25 cells can promote ferroptosis by increasing reactive oxygen species, MDA, and iron content, and downregulating GPX4 expression[45]. This was consistent with our results that FGF6 can upregulate the expression of GPX4 and ACSL4 in the ferroptosis pathway, thereby inhibiting ferroptosis in OSCC.

In summary, we explored the role of FGF6 in the progression of OSCC at the protein and transcriptional levels and found that it may mediate the PI3K-AKT and MAPK pathways to regulate the progression of OSCC, providing new ideas for early clinical diagnosis and new targets for treatment. However, this study has some limitations. First, there is a difference in age due to some uncontrollability in the collection of clinical specimens. But to control for this bias, we constructed the animal model to verify the results. Second, additional experiments such as changes in downstream MAPK and PI3K signaling pathways after FGFR4 knockdown are needed to further support this conclusion. And whether FGF6 can be used to diagnose OSCC is still unknown, and a large number of clinical sample tests are needed to verify this. The future development of an FGF6 inhibitor drug may be promising for controlling OSCC progress.

Conclusion

FGF6 may upregulate the phosphorylation level and change the expression of related apoptosis proteins and proliferation factors by binding to FGFR4 in the PI3K-AKT/MAPK pathway and may inhibit the ferroptosis of OSCC, thereby possibly participating in the process of inhibiting OSCC.

Data availability

The datasets generated and/or analyzed during the current study are not publicly available but are available from the corresponding author upon reasonable request.

Received: 21 June 2024; Accepted: 31 October 2024
Published online: 06 November 2024

References

1. Menditti, D. et al. Personalized medicine in oral oncology: Imaging methods and biological markers to support diagnosis of oral squamous cell carcinoma (OSCC): A narrative literature review. *J. Pers. Med.* **13**, (2023).
2. Shen, T. et al. BTC as a novel biomarker contributing to EMT via the PI3K-AKT pathway in OSCC. *Front. Genet.* **13**, 875617 (2022).
3. Truchard, E. et al., Identification of a gene-expression-based surrogate of genomic instability during oral carcinogenesis. *Cancers (Basel) 14*, (2022).
4. Chettiankandy, T. J. et al. Role of nidogen-2 in diagnosis and prognosis of head and neck squamous cell carcinoma: A systematic review. *J. Oral Maxillofac. Pathol.* **26**, 382–388 (2022).
5. Lodi, G. et al. Interventions for treating oral leukoplakia to prevent oral cancer. *Cochrane Database Syst. Rev.* **7**, Cd001829 (2016).
6. Wang, S., Yang, M., Li, R. & Bai, J. J. E. J. M. R. Current advances in noninvasive methods for the diagnosis of oral squamous cell carcinoma: A review. **28**, 1–12 (2023).
7. Chai, A. W. Y., Lim, K. P. & Cheong, S. C. (eds) *Translational Genomics and Recent Advances in Oral Squamous Cell Carcinoma. Seminars in Cancer Biology* (Elsevier, 2020).
8. Prakash, N. & Pradeep, G. J. J. O. JOMFP MP. Circulating biomarkers in oral cancer: Unravelling the mystery. **26**, 300 (2022).
9. Rapado-González, Ó. et al., Integrity and quantity of salivary cell-free DNA as a potential molecular biomarker in oral cancer: A preliminary study. **51**, 429–435 (2022).
10. Araujo, A. L. D., Santos-Silva, A. R. & Kowalski, L. P. J. C. O. R. Diagnostic accuracy of liquid biopsy for oral potentially malignant disorders and head and neck cancer: An overview of systematic reviews. **25**, 279–292 (2023).
11. Casagrande, G. M. S., Silva, M. O., Reis, R. M. & Leal, L. F. J. I. J. M. S. Liquid biopsy for lung cancer: Up-to-date and perspectives for screening programs. **24**, 2505 (2023).
12. Alimirzaie, S., Bagherzadeh, M. & Akbari, M. R. J. C. Liquid biopsy in breast cancer: A comprehensive review. **95**, 643–660 (2019).

13. Wills, B., Gorse, E. & Lee, V. J. C. P. C. Role of liquid biopsies in colorectal cancer. **42**, 593–600 (2018).
14. Armand, A-S. & Laziz, I. Chanoine CJBeBA-MCR. FGF6 in myogenesis. **1763**, 773–778 (2006).
15. Othman, A., Mubarak, R. & Sabry, D. J. F. Fibroblast growth factor-6 enhances CDK2 and MATK expression in microvesicles derived from human stem cells extracted from exfoliated deciduous teeth. **7**, (2018).
16. Herrmann, A. et al. Pipeline for large-scale microdroplet bisulfite PCR-based sequencing allows the tracking of hepitype evolution in tumors. **6**, e21332 (2011).
17. Zhi, Y. et al. LINC00265 promotes the viability, proliferation, and migration of bladder cancer cells via the miR-4677-3p/FGF6 axis. **40**, S434–S446 (2021).
18. Guo, S. et al. A gene-based recessive diplotype exome scan discovers FGF6, a novel hepcidin-regulating iron-metabolism gene. **133**, 1888–1898 (2019).
19. Singhi, A. D. et al. Real-time targeted genome profile analysis of pancreatic ductal adenocarcinomas identifies genetic alterations that might be targeted with existing drugs or used as biomarkers. **156**, 2242–2253. e2244 (2019).
20. Wheler, J. J. et al. Presence of both alterations in FGFR/FGF and PI3K/AKT/mTOR confer improved outcomes for patients with metastatic breast cancer treated with PI3K/AKT/mTOR inhibitors. **3**, 164 (2016).
21. Acevedo, V. D., Ittmann, M. & Spencer, D. M. Paths of FGFR-driven tumorigenesis. *Cell. Cycle* **8**, 580–588 (2009).
22. Guo, C-H. et al. Fish oil and selenium with doxorubicin modulates expression of fatty acid receptors and selenoproteins, and targets multiple anti-cancer signaling in triple-negative. *Breast Cancer Tumors* **19**, 2044 (2022).
23. Noorolyai, S., Shajari, N., Baghbani, E., Sadreddini, S. & Baradaran, B. J. G. The relation between PI3K/AKT signalling pathway and cancer. **698**, 120–128 (2019).
24. Fruman, D. A. et al. The PI3K pathway in human disease. **170**, 605–635 (2017).
25. Revathidevi, S. & Munirajan, A. K. (eds) *Akt in Cancer: Mediator and More. Seminars in Cancer Biology* (Elsevier, 2019).
26. Lakshminarayana, S. et al. Molecular pathways of oral cancer that predict prognosis and survival: A systematic review. **17**, (2018).
27. Singh, R., Letai, A. & Sarosiek, K. J. N. M. Regulation of apoptosis in health and disease: The balancing act of BCL-2 family proteins. **20**, 175–193 (2019).
28. Feng, J. et al. CLIC1 promotes the progression of oral squamous cell carcinoma via integrins/ERK pathways. **11**, 557 (2019).
29. Barbosa, R., Acevedo, L. A. & Marmorstein, R. J. M. C. R. The MEK/ERK network as a therapeutic target in human cancer. **19**, 361–374 (2021).
30. Wang, S. et al. RN181 is a tumour suppressor in gastric cancer by regulation of the ERK/MAPK–cyclin D1/CDK4 pathway. **248**, 204–216 (2019).
31. Su, X. et al. Vitamin C kills thyroid cancer cells through ROS-dependent inhibition of MAPK/ERK and PI3K/AKT pathways via distinct mechanisms. **9**, 4461 (2019).
32. Li, H. et al. HLF regulates ferroptosis, development and chemoresistance of triple-negative breast cancer by activating tumor cell-macrophage crosstalk. **15**, 1–6 (2022).
33. Ouyang, S. et al. Inhibition of STAT3-ferroptosis negative regulatory axis suppresses tumor growth and alleviates chemoresistance in gastric cancer. **52**, 102317 (2022).
34. Gu, W. et al. Multi-omics analysis of ferroptosis regulation patterns and characterization of tumor microenvironment in patients with oral squamous cell carcinoma. **17**, 3476 (2021).
35. Kanehisa, M. & Goto, S. KEGG: kyoto encyclopedia of genes and genomes. *Nucleic Acids Res.* **28**, 27–30 (2000).
36. Kanehisa, M. Toward understanding the origin and evolution of cellular organisms. *Protein Sci.* **28**, 1947–1951 (2019).
37. Kanehisa, M., Furumichi, M., Sato, Y., Kawashima, M. & Ishiguro-Watanabe, M. KEGG for taxonomy-based analysis of pathways and genomes. *Nucleic Acids Res.* **51**, D587–d592 (2023).
38. Penault-Llorca, F. et al. Expression of FGF and FGF receptor genes in human breast cancer. **61**, 170–176 (1995).
39. Kwabi-Addo, B., Ozen, M. & Ittmann, M. J. E. The role of fibroblast growth factors and their receptors in prostate cancer. **11**, 709–724 (2004).
40. Floss, T., Arnold, H-H. & Braun, T. J. G. Development. A role for FGF-6 in skeletal muscle regeneration. **11**, 2040–2051 (1997).
41. Katayama, Y. et al. Tumor neovascularization and developments in therapeutics. *Cancers (Basel)* **11** (2019).
42. Yehya, A. H. S. et al. Angiogenesis: Managing the culprits behind tumorigenesis and metastasis. *Medicina (Kaunas)* **54** (2018).
43. El Hanbuli, H. M. & Abou Sarie MAJIJoP. KRAS protein expression in oral squamous cell carcinoma: A potential marker for progression and prognosis. **17**, 469 (2022).
44. Aziz, M. M. A., Zaki, M. M., Farg, D. A. & El Kourdy, K. A. J. E. J. P. Immunohistochemical expression of Bcl-2 in oral squamous cell carcinoma: A clinicopathological correlation. **39**, 257 (2019).
45. Sun, K. et al. MiR-34c-3p upregulates erastin-induced ferroptosis to inhibit proliferation in oral squamous cell carcinomas by targeting SLC7A11. **231**, 153778 (2022).

Acknowledgements

Not Applicable.

Author contributions

X.L. conceived and designed the study; M.N. provided the administrative support; X.L., Y.X., and L.S. provided materials and samples; X.L., X.Z., M.H., and M.Z. collected and assembled data; X.L. and X.C. analyzed and interpreted the data; All authors have read and approved the final manuscript.

Funding

This study was supported by the National Natural Science Foundation of China (82401112), the Open Project of National Key Laboratory of Oral Disease Prevention and Treatment (SKLOD2024OF04), and the Science and Technology Innovation Talent Program of Luzhou Science and Technology Knowledge Bureau (2023RCX171).

Declarations

Competing interests

The authors declare no competing interests.

Ethical approval

The study was reviewed and approved by all procedures were approved by medical Ethics Committee of Affiliated Stomatological Hospital of Southwest Medical University (Permit Number: 20180510001). The animal study was reviewed and approved by all procedures were approved by the Southwest Medical University

Animal Ethics Committee (Permit Number: 2020435).

Consent for publication

Not applicable.

Additional information

Supplementary Information The online version contains supplementary material available at https://doi.org/10.1038/s41598-024-78552-7.

Correspondence and requests for materials should be addressed to M.N. or X.L.

Reprints and permissions information is available at www.nature.com/reprints.

Publisher's note Springer Nature remains neutral with regard to jurisdictional claims in published maps and institutional affiliations.